

1 **Manuscript No. JFOODENG-D-20-01421r1**

2 **Research Article**

3

4 **Title: Crystallization Characteristics of Amorphous Trehalose Dried**
5 **from Alcohol**

6

7

8 Authors: Takanari Sekitoh^a, Takashi Okamoto,^a Akiho Fujioka,^a Tomohiko Yoshioka,^b

9 Shinji Terui,^b Hiroyuki Imanaka,^a Naoyuki Ishida,^a and Koreyoshi Imamura^{a,*}

10

11 ¹ Division of Chemistry and Biochemistry, Graduate School of Natural Science and
12 Technology, Okayama University, 3-1-1 Tsushima-naka, Kita-ku, Okayama 700-8530,

13 Japan

14 ² Graduate School of Interdisciplinary Science and Engineering in Health Systems,
15 Okayama University, 3-1-1 Tsushima-naka, Kita-ku, Okayama 700-8530, Japan

16

17 *Correspondence concerning this article should be addressed to K. Imamura

18 E-mail: kore@cc.okayama-u.ac.jp

19

20 Running Title: ANHYDROUS CRYSTALLIZATION OF TREHALOSE

21

22

23

24

25 **ABSTRACT**

26

27 Trehalose forms a glass that can be used to preserve labile substances under desiccation.
28 The crystallization characteristics, namely crystallization temperature (T_{cry}) and
29 isothermal crystallization behavior of amorphous trehalose, dried from alcohol
30 (methanol, ethanol), was analyzed and the results were compared with those for the
31 amorphous trehalose freeze-dried from water. The use of alcohol as a drying solvent
32 lowered the T_{cry} by $\sim 90^{\circ}\text{C}$ from the value for the case of an aqueous solvent. The
33 formation of multiple forms of crystals and partial melting were suggested by the
34 thermal analysis. Isothermal crystallization experiments showed that the
35 alcohol-originated amorphous trehalose was eventually exclusively converted into
36 β -form crystals. The induction period (t_{ind}) before the start of isothermal
37 crystallization was markedly shortened when alcohol was used as the solvent compared
38 to water. The t_{ind} values for various amorphous sugar samples including the
39 alcohol-originated ones could be correlated with difference between T_{cry} and the sample
40 temperature.

41

42 Key words: trehalose, crystallization, anhydrous crystal, methanol, vacuum foam drying

43

44

45 1. Introduction

46

47 Trehalose (1-O- α -D-glucopyranosyl- α -D-glucopyranoside) is used as a stabilizing
48 agent and an excipient in the food and pharmaceutical industries (Crowe, 2007; Elbein,
49 Pan, Pastuszak, & Carroll, 2003; Jain, Roy, 2009; Kopjar et al., 2013; Neri et al., 2014;
50 Ohtake & Wang, 2011; Umene, Hayashi, Kato, & Masunaga, 2015), and the
51 commercial usage of trehalose appears to be increasing year by year (Cai et al., 2018;
52 Walayat et al., 2020). Trehalose is commonly available in the form of a dihydrate
53 crystalline material. The procedures and conditions for preparing crystalline trehalose
54 dihydrate was commercially established (Kubota, Sawatani, Oku, Takeuchi, & Murai,
55 2004; Schiraldi, Di Lernia, & De Rosa, 2002).

56 Trehalose can exist in the form of anhydrous crystals and the crystallization
57 behavior of trehalose under anhydrous conditions has been extensively investigated
58 (Nagase et al., 2008; Ohashi, Yoshii, & Furuta, 2007a; Ohashi, Yoshii, & Furuta, 2007b;
59 Pyszczynski & Munson, 2013; Sussich, Urbani, Princivalle, & Cesàro, 1998). The
60 β -form of trehalose crystals can be produced by heating dihydrate crystals at 85°C under
61 a vacuum (Nagase, Endo, Ueda, & Nagasaki, 2002) or at 70°C in ethanol containing
62 2.5% water (Verhoeven et al., 2012). Amorphous trehalose, vacuum dried from an
63 aqueous solution, was also converted into the anhydrous crystal in the α -form (Reisener,
64 Goldschmid, Ledingham, & Perlin, 1962) while spray-dried (Surana, Pyne, &
65 Suryanarayanan, 2004) or freeze-dried amorphous trehalose (Roe, & Labuza, 2005)
66 does not undergo crystallization under anhydrous conditions. In addition, the aging of
67 amorphous trehalose was found to facilitate the crystallization of the anhydrous form of
68 trehalose (Surana, Pyne, & Suryanarayanan, 2004).

69 It should be noted that our previous study demonstrated that, when a sugar is
70 amorphized somehow such as by the freeze-drying of an aqueous solution, the solubility
71 of the resulting amorphous sugar in a simple alcohol such as methanol was much
72 greater than the equilibrium solubility of the material (Sato et al., 2016). An organic
73 solution containing sugar can be converted into an amorphous sugar powder by
74 allowing it to dry up before the occurrence of segregation. The alcohol-originated
75 amorphous sugars have significantly lower glass transition temperatures than
76 corresponding samples dried from an aqueous solution (Takeda et al., 2017) and thus
77 would also be expected to show different crystallization characteristics.

78 This study reports on an examination of the crystallization characteristics of
79 amorphous trehalose, dried from an organic solvent, as well as their glass transition
80 behavior. Amorphous trehalose was prepared by drying an alcohol solution of

81 trehalose and the glass transition temperature (T_g), crystallization temperature (T_{cry}) and
82 crystallization processes of the material under different conditions as well as the crystal
83 form of crystallized trehalose were determined. Interactions between trehalose
84 molecules in the dried amorphous matrix were also analyzed and the findings were
85 compared between different types of solvent.

86

87 **2. Materials and methods**

88

89 *2.1. Materials*

90

91 Methanol and ethanol, used as solvent, were purchased from Wako Pure Chemicals
92 Industries Ltd. (Osaka, Japan). Trehalose was a product of Nacalai Tesque Inc. (Kyoto,
93 Japan). Dihydrate trehalose crystal powder was dissolved in distilled water to give a
94 final concentration of 100 mg/mL. A 10 mL ~~solution~~ of a trehalose solution was
95 frozen in a freezer (-20°C) and further cooled in liquid nitrogen for ~5 min to give a
96 completely frozen sample. The frozen samples were freeze-dried, as described in our
97 previous study (Imamura et al., 2008a). Our previous studies showed that the resulting
98 freeze-dried matrix of trehalose is fully amorphous (Takeda et al., 2017). The
99 freeze-dried cake of amorphous trehalose was thoroughly dehydrated by storage under a
100 vacuum over P₂O₅ at 37°C for more than three days. The attained residual water
101 content of the amorphous trehalose cake was below the detection limit (>0.002 g/g-dry
102 matter) based on a Karl-Fischer titration analysis (Takeda et al., 2017).

103

104 *2.2. Vacuum foam drying*

105

106 A 10 ~~ten~~ mL portion of methanol was added to a glass vial that contained 1 g of
107 amorphized trehalose cake and vigorously shaken with a vortex mixer for 10 seconds to
108 homogeneously disperse (dissolve) the trehalose in methanol. Aliquots of 100 µL of
109 the organic solution were transferred to 1.5 mL polypropylene sampling tubes and then
110 vacuum-dried at ca. 1000 Pa for 90 min (initial drying) using a centrifugal concentrator
111 (EYELA CVE-1100, TOKYO RIKAKIKAI Co., Tokyo, Japan) connected to a
112 diaphragm type vacuum pump (FDU-1200, ULVAC Japan, Ltd., Tokyo, Japan). The
113 foaming of the solution was not induced during the initial drying. After the initial
114 drying, the sample solution was removed from the centrifugal concentrator and then
115 punctured with a stainless steel needle (Hidaka et al., 2019; Satoh et al., 2017), followed
116 by further vacuum drying (Second drying) for 30 min. The needle puncturing

117 (stimulation) reliably induced foaming immediately after the start of the secondary
118 drying. The amount of the remaining organic solvent in the dried sample was
119 estimated to be less than 0.01 g/g-dry matter, based on drying profiles reported in our
120 previous study (Hidaka et al., 2019; Satoh et al., 2017).

121

122 *2.3. Differential scanning calorimetry*

123

124 Differential scanning calorimetry (DSC) analyses of amorphous trehalose samples,
125 obtained from alcohols (methanol, ethanol) as well as water, were conducted, using a
126 TA Q2000 calorimeter (TA instruments Co., New Castle, DE) equipped with RCS90
127 cooling system (TA instruments Co.) according to the same procedures as was used in
128 our previous study (Sekitoh et al., 2021; Takeda et al., 2017; Takeda et al., 2019).
129 Namely, 1~5 mg of an amorphous trehalose sample was hermetically sealed in an
130 aluminum pan and then scanned from -40°C to 190°C at a rate of 10°C/min, in which an
131 empty aluminum pan was used as a reference. The glass transition temperature of the
132 sample, T_g , was determined as the onset of heat capacity change in the obtained DSC
133 curve. The prewarming of the sample was omitted since it has been known to alter the
134 characteristics of the amorphous sugar matrix dried from alcohol (Sekitoh et al., 2021;
135 Takeda et al., 2019).

136

137 *2.4. Powder x-ray diffractometry*

138

139 The amorphous trehalose sample that had been dried from methanol (and then
140 sealed in a DSC pan) was stored at 80°C for 60 min to fully crystallize (isothermal
141 crystallization). The resulting heated sample as well as the unheated sample were
142 pulverized into fine powders and then placed on a sample holder of an X-ray
143 diffractometer PANalytical X'PERT PRO MPD system with Cu-K α radiation
144 (PANalytical B.V., Almelo, Holland). X-ray diffraction spectra of the trehalose
145 samples were measured at an X-ray tube voltage of 45 kV and a current of 40 mA.
146 The trehalose samples, dried from alcohols or water and without being heated, were also
147 analyzed by XRD and confirmed to be fully amorphous.

148

149 *2.5. Fourier transform infrared ray spectroscopy*

150

151 IR absorption spectra of amorphous trehalose samples that had been dried from
152 different solvents were obtained using a Fourier transform IR spectrometer (FTIR,

153 Nicolet 4700, Thermo Scientific Inc., Madison, WI) with a diffuse diffraction technique
154 in the same manner as was used in our previous study (Imamura et al., 2008b).
155 Namely, a 1~2 mg sample of amorphous sugar was ground into a fine powder with an
156 approximately 100-fold amount of powdered KBr. The resulting mixed powder was
157 packed in a stainless steel cup for the diffuse reflection attachment (Gemini, Spectra
158 Tech., Co., Shelton, CT) and then scanned 64 times from 600 cm^{-1} to 4000 cm^{-1} at a
159 resolution of 4 cm^{-1} .

160 The extents of formation of sugar-sugar hydrogen bonds in different amorphous sugar
161 samples can be semi-quantitatively compared based on the peak frequency of the sugar
162 O-H stretching vibration bands (Imamura et al., 2006; Kagotani et al., 2013; Takeda et
163 al., 2019; Wolkers, van Kilsdonk, & Hoekstra, 1998). Hence, the measured IR spectra
164 for dried amorphous trehalose samples were smoothed at 80 points and the peak
165 wavenumber of the IR band due to sugar O-H stretching vibration was determined at
166 around 3300 cm^{-1} (Kagotani et al., 2013; Takeda et al., 2019).

167 The FTIR measurement were at least triplicated for each sample, and the deviations
168 in wavenumber was within 5 cm^{-1} of the average values.

169

170 **3. Results and discussion**

171

172 *3.1. DSC measurements*

173

174 The thermograms of amorphous trehalose samples, prepared by vacuum foam
175 drying from alcohols and freeze-drying from water, are shown in Fig. 1. A single shift
176 in the apparent heat capacity of the sample, corresponding to the glass-to-rubber
177 transition, was detected in all the amorphous trehalose samples. The glass transition
178 temperatures, T_g , for the trehalose samples were determined from the DSC thermograms
179 and the results are listed in Table 1. As shown in Table 1, the T_g value of amorphous
180 trehalose matrix is varied depending on the solvent. Namely, the T_g for the
181 freeze-dried amorphous trehalose **obtained from the aqueous solution** was around 105
182 $^{\circ}\text{C}$, which is in good agreement with previously reported values (Imamura et al., 2008c;
183 Miller & de Pablo, 2000; Roos, 1993; Saleki-Gerhardt & Zograf, 1994; Surana, Pyne,
184 & Suryanarayanan, 2004) although some data showed slightly higher ($\sim 10^{\circ}\text{C}$) values
185 (Miller & de Pablo, 2000; Saleki-Gerhardt & Zograf, 1994; Surana, Pyne, &
186 Suryanarayanan, 2004); The methanol- and ethanol-**solutions** originated samples
187 exhibited ~ 50 and $\sim 30^{\circ}\text{C}$ lower T_g than the water-originated ones.

188 The amorphous trehalose samples dried from alcohols exhibited an exothermic peak
189 at temperatures that were 30~50°C higher than T_g (curves (a) and (b) in Fig. 1) as well
190 as an endothermic peak in the temperature range above ~170°C. These exothermic
191 and endothermic peaks are assumed to be due to the crystallization and melting of
192 trehalose, respectively. It should be noted that the thermograms for the methanol- and
193 ethanol-originated samples exhibited an at-least-three-dented bottom of the 170~200°C
194 endothermic peak. This indicates that multiple forms of crystals are formed in the
195 DSC upward scan, which has also been indicated in a previous study (Nagase et al.,
196 2008; Pyszczyński & Munson, 2013; Sussich, Urbani, Princivalle, & Cesàro, 1998).

197 In the case of water as a solvent, the two exo- and endothermic peaks were
198 significantly overlapped with each other. This results in markedly small ΔH_{cry} and
199 ΔH_m values (Table 1), relative to those for the case of water as the solvent. Assuming
200 that the ΔH_m for the water solvent is equal to the reported value (~156 J/g) (Cai et al.,
201 2018; Jain & Roy, 2009), the overlapping magnitude is estimated to be approximately
202 130 J/g. It thus follows that the true value for the ΔH_{cry} for the water-originated
203 sample would likely be around 150 J/g, which is in agreement with the reported value
204 (~140 J/g) (Surana, Pyne, & Suryanarayanan, 2004). Compared to the true ΔH_{cry} value
205 for the water solvent, the ΔH_{cry} values for the alcohol-originated samples were markedly
206 low, implying that the corresponding exotherm involves not only (multiple forms of)
207 trehalose crystallization but also melting. Actually, in the thermogram for the
208 methanol-originated sample, the exotherm is accompanied by a small endothermic peak,
209 which may be due to the endotherm for the melting of crystallized trehalose in the α
210 ($T_m=120^\circ\text{C}$) (Pyszczyński & Munson, 2013; Sussich, Urbani, Princivalle, & Cesàro,
211 1998) and γ forms (Sussich, Urbani, Princivalle, & Cesàro, 1998)).

212 The onset temperatures (T_{cry} and T_m) and heats of the exothermic (ΔH_{cry}) and
213 endothermic peaks (ΔH_m) as well as the reported values (Pyszczyński & Munson, 2013;
214 Surana, Pyne, & Suryanarayanan, 2004; Sussich, Urbani, Princivalle, & Cesàro, 1998)
215 are listed in Table 1. The data shown in Table 1 **indicate** indicates that the use of
216 methanol or ethanol as a drying solvent significantly lowers the T_{cry} value and therefore
217 facilitates the crystallization of trehalose, compared to the case of water as the solvent.
218 The T_{cry} for the methanol-originated sample is slightly lower than that for the
219 ethanol-originated one. The melting enthalpy, ΔH_m for the case where the sample was
220 dried from alcohols is in the range of 140~160 J/g. This is entirely consistent with the
221 reported value (Cai et al., 2018; Jain & Roy, 2009) and also roughly comparable to the
222 melting enthalpy of sucrose (134 J/g) (Hurttta, Pitkanen, & Knuutinen, 2004) although

223 the existence of different forms of trehalose crystals was suggested by the DSC
224 thermogram (Fig. 1), as described above.

225 Figure 2 shows the IR absorption O-H stretching vibration ($\nu_{\text{O-H}}$) bands for
226 amorphous trehalose samples dried from different solvents. As shown in Fig. 2, the
227 methanol-originated sample showed considerably lower peak wavenumbers for the $\nu_{\text{O-H}}$
228 band than the other two, suggesting a greater extent of hydrogen bond formation. The
229 $\nu_{\text{O-H}}$ band for the ethanol-originated sample is positioned at a slightly higher frequency
230 than that of the methanol-originated one (Fig. 2).

231 Our previous study suggested that the specific molar volume of a disaccharide
232 (α -maltose) in methanol was approximately 30% smaller than that in water (Takeda et
233 al., 2019). Trehalose molecules are also considered to have markedly smaller
234 occupied volumes in alcohols than in water and possibly retain highly packed
235 conformations, even when thoroughly dried (from alcohols). Consequently, the
236 intimate hydrogen bonding may be an important feature of the amorphous trehalose
237 matrix dried from alcohols by the smaller occupied volume of trehalose molecules, as
238 indicated by the lower peak wavenumbers of the $\nu_{\text{O-H}}$ band (Fig. 2).

239 When the methanol- and ethanol-originated samples are compared, the T_g , T_{cry} and
240 IR peak wavenumbers of the $\nu_{\text{O-H}}$ band are slightly higher in the case where methanol is
241 used as a drying solvent than in the case of ethanol while they are clearly lower than
242 when dried from water (Table 1 and Fig. 2). Although detailed reasons for this are
243 unknown at the present stage, this may possibly be related to the molar bulk densities of
244 methanol and ethanol. Namely, ethanol has ca. a 44% smaller molar density (17.2
245 mmol/mL) than methanol (24.7 mmol/mL) (Merck index No. 5816 and 212, 10th ed),
246 which might allow trehalose molecules to be less packed in ethanol than in methanol.
247 Consequently, intermediate characteristics between those of the methanol- and
248 water-originated samples might be exhibited when ethanol was used as the drying
249 solvent.

250 Considering the findings obtained from the FTIR analysis (Fig. 2) and based on the
251 “free volume theory (Boyer & Spencer, 1944; Frenkel, 1955),” the markedly lower T_g
252 value for the alcohol-originated samples than that for the water-originated samples can
253 be explained as follows. Namely, the dependence of the specific molar volume of the
254 trehalose molecule on temperature can be schematically represented by two lines,
255 corresponding to glassy and rubbery states as shown in Fig. 3, and the crossing point
256 temperature is the T_g value for amorphous trehalose. As described above, the specific
257 volume of trehalose molecules in the alcohol-originated amorphous matrix is considered
258 to be smaller than that in the water-originated sample, which would shift the line for the

259 glassy state downward (dotted line in Fig. 3). Assuming that the specific molar
260 volume in the rubbery state is independent of the solvent type, it follows that the
261 crossing point between the glassy- and rubbery-state lines (namely T_g) will shift toward
262 lower temperature (Fig. 3).

263

264 3.2. Isothermal crystallization behavior

265

266 As indicated by Fig. 1, the crystallization of an amorphous trehalose matrix is
267 markedly facilitated when it is first dried from methanol and ethanol. Hence, we next
268 conducted isothermal crystallization tests of the alcohol- and water-originated
269 amorphous trehalose. Figure 4 shows XRD patterns for the amorphous trehalose
270 sample that had been vacuum foam dried from methanol and then heated for 60 min at
271 80°C. The resulting XRD spectrum after the isothermal crystallization test indicates
272 the presence of several sharp peaks, and the peak positions are completely consistent
273 with those for β form of anhydrous crystals of trehalose (Sussich, Urbani, Princivalle, &
274 Cesàro, 1998). This suggests that β -form of trehalose anhydrous crystal is exclusively
275 obtained in the isothermal crystallization. However, when the entire crystallization
276 exotherm was integrated during the isothermal crystallization test, the value was found
277 to be ca. 37±5 J/g, which is approximately one fourth that for ΔH_m and even less than
278 the ΔH_{cry} (Table 1). The isothermal crystallization of anhydrous trehalose therefore
279 appears to involve multiple thermal events, including the formation of multiple forms of
280 trehalose crystals and their subsequent melting, although all of the trehalose molecules
281 are eventually converted into the β form. This insight is consistent with the
282 observation for the ascending **DSC scanning** (Fig. 1 and Table 1).

283 The isothermal crystallization processes of the amorphous trehalose samples are
284 shown in Fig. 5. The crystallization processes were approximated by using the
285 following modified Avrami equation (Avrami, 1939; Avrami, 1940; Avrami, 1941;
286 Erofeev, 1946; Imamura et al., 2010; Imamura, Kinugawa, Kagotani, Nomura, &
287 Nakanishi, 2012; Kedward, MacNaughtan, Blandshard, & Mitchell, 2008; Kedward,
288 MacNaughtan, & Mitchell, 2000), having the induction period, t_{ind} (min):

289

$$290 \quad C(t) = \exp[-\{k_{cry}(t-t_{ind})\}^n] \quad (1)$$

291

292 where $C(t)$ denotes the degree of crystallinity at the time point of t (min), and k_{cry} and n
293 are originally regarded as the rate constant and dimension of crystal growth,
294 respectively (Avrami, 1939; Avrami, 1940; Avrami, 1941; Erofeev, 1946). The kinetic

295 parameters for the crystallization of the different samples and temperatures were
296 determined by the Avrami plot of $\ln C(t)$ vs $\ln(t-t_{\text{ind}})$ (Fig. 5(b)) and the results are
297 summarized in Table 2. As shown in Table 2, the induction time for the crystallization,
298 t_{ind} , is drastically shortened with increasing temperature. It should be noted that the t_{ind}
299 values for the methanol- and ethanol-originated samples are in the same range as those
300 for the water originated sample (Table 2) irrespective of the significantly lower tested
301 temperature range. This demonstrates that the use of alcohols as a solvent significantly
302 facilitates crystal nucleation.

303 On the other hand, since the multiple thermal events including crystallization and
304 melting may occur during isothermal crystallization, as described above, the obtained k_{cl}
305 and n values are only qualitative rather than reflecting the actual crystal growth kinetics.
306 However, the determined n values are roughly 5 ± 1 (-), except for the case of water as a
307 solvent and heating temperature of 170°C (Table 1 and Fig. S1(a)). These large n
308 values (>4) may be attributed to the overlapping of multiple phase transitions of
309 trehalose that can allow the increase in the “specific” surface area of the crystal phase
310 with the advance of the crystallization (Ohashi, Yoshi, & Furuta, 2007b). The
311 isothermal crystallization of water-originated amorphous trehalose shows an
312 exceptionally small $k_{\text{cry}} n$ value at 170°C (3.2 ± 0.4), which may possibly be related to the
313 testing temperature being quite close to the T_{m} value (Table 1).

314 The crystal growth rate has been accepted to increase with $(T-T_{\text{g}})$ value (Truong &
315 Wang, 2017). However, the plot of k_{cry} values (Table 2) as a function of $(T-T_{\text{g}})$ (Fig.
316 S1(b)) exhibits clearly different curves for each solvent although the k_{cl} value for each
317 solvent-originated sample usually increases with increasing $(T-T_{\text{g}})$. This finding may
318 suggest that the crystal growth kinetics is strongly affected by the solvent type and thus
319 trehalose molecule conformation before being dried. The exceptionally small k_{cl} value
320 for water-originated amorphous trehalose at $(T-T_{\text{g}})=63^\circ\text{C}$ (Fig. S1(b)) may be due to the
321 melting overlapped to crystallization, similarly to the small n value (3.2 ± 0.4) as
322 described above.

323 The amorphous sugar matrix, obtained by the freeze-drying the aqueous solution of
324 sugar, is comprised of pores and thin pore walls (a few micrometers in thickness)
325 (Abdul-Fattah, 2007; Imamura et al., 2010), and the pore walls contain huge cavities that
326 take up (sorb) water molecules (Imamura, Kagotani, Nomura, Kinugawa, & Nakanishi,
327 2012; Kagotani et al., 2013). Our previous study demonstrated that, when compressed
328 at several hundred MPa, the pores and cavities in freeze-dried amorphous sugar are
329 reduced and, concomitantly, the t_{ind} is markedly shortened (Imamura et al., 2010;
330 Imamura, Kinugawa, Kagotani, Nomura, & Nakanishi, 2012). Based on these findings,

331 we conclude that the matrix pores and cavities may serve as a discontinuous area that
332 interferes with the nucleation of sugar crystals and subsequent growth; The continuity
333 of the sugar matrix is increased when the matrix pores and cavities are diminished due
334 to the compression, resulting in sugar crystallization being facilitated (Imamura,
335 Kinugawa, Kagotani, Nomura, & Nakanishi, 2012). On the other hand, in the case of
336 vacuum foam drying, the sugar in alcohol exists in the dissolved (liquid) and rubbery
337 state until it is converted into a glassy solid (Hidaka et al., 2019). The flowable state
338 of a sugar solution during vacuum foam drying is thought to result in minimizing the
339 discontinuities in the sugar matrix and thus facilitate the subsequent crystallization of
340 the sugar. Consequently, the amorphous trehalose, vacuum-foam-dried from alcohol,
341 may exhibit markedly a smaller t_{ind} value (Table 2) as well as a lower T_{cry} than a sample
342 that was freeze-dried from water (Table 1).

343 Our previous studies revealed that the induction period before the crystallization for
344 amorphous sucrose and α -lactose, prepared by freeze-drying, could be correlated with
345 the difference between the crystallization temperature (T_{cry}) and the sample temperature
346 (Imamura, Kinugawa, Kagotani, Nomura, & Nakanishi, 2012; Kinugawa et al., 2015).
347 Figure 6 summarizes the t_{ind} values for the amorphous trehalose samples prepared in
348 this study as well as those for freeze-dried amorphous sucrose and lactose. As shown
349 in Fig. 6, the t_{ind} values for amorphous trehalose that was dried from different solvents,
350 are plotted around the curve representing the $t_{\text{ind}}-(T_{\text{cry}}-T)$ relationship for sucrose and
351 α -lactose (Imamura, Kinugawa, Kagotani, Nomura, & Nakanishi, 2012; Kinugawa et al.,
352 2015). Accordingly, the induction period for crystallization can be predicted from the
353 T_{cry} value, irrespective of the type of the original solvent used as well as the sugar type.

354 The T_{cry} can be regarded as the temperature at which a critical nucleus that can grow
355 is formed without any delay, and the probability for the critical nucleus formation is
356 thus expected to decrease with decreasing temperature; In principle, when the sample
357 temperature is lowered to T_g , the induction period would become infinite. Considering
358 these, the existence of a common relationship between t_{ind} and $(T_{\text{cry}}-T)$ would mean
359 that the decrease in t_{ind} with increasing sample temperature from T_g to T_{cry} is in the same
360 order, irrespective of the type of solvent and sugar type as well as water sorption state,
361 etc.

362 Our previous study (Sekitoh et al., 2021; Takeda et al., 2019) indicated that the
363 thermal annealing of the amorphous sugar, vacuum foam dried from alcohols, markedly
364 increased the T_g value. Considering this, the T_{cry} also is expected to be altered by
365 thermal annealing, and furthermore, the temperature where amorphous sugar is
366 solidified, namely drying temperature, may change (increase) the T_g and possibly T_{cry}

367 values. Further study on the influence of the drying condition (especially, drying
368 temperature) on the thermal characteristics of the amorphous trehalose matrix is
369 required to increase the options to produce the amorphous sugar-based products.

370

371 **4. Conclusions**

372

373 Amorphous trehalose was prepared by vacuum foam drying from alcohols
374 (methanol and ethanol), and the T_g , T_{cry} , and crystallization behavior of the samples
375 were compared with those for aqueous freeze-dried trehalose. The trehalose samples
376 produced from methanol and ethanol showed markedly lower T_g values than the
377 water-originated sample, which can be explained by their high molecular packing states,
378 as evidenced by FTIR analysis. The T_{cry} and induction periods (t_{ind}) before the start of
379 the isothermal trehalose crystallization were markedly lower and shorter in the case of
380 samples that were dried from alcohols compared to samples that were freeze-dried from
381 water. This indicates that the use of alcohol as a solvent facilitates the formation of the
382 critical nucleus of anhydrous trehalose crystal that can then grow. Plots of t_{ind} against
383 ($T-T_{cry}$) for the amorphous trehalose obtained from different solvents (methanol, ethanol,
384 and water) coincide well with those reported for different sugar types, sample
385 treatments (rehumidification and compression), and related processes. The isothermal
386 crystallization eventually exclusively produced β form crystals, but different types of
387 anhydrous trehalose crystals appear to have been temporarily produced during the
388 overall process. Hence, for an understanding of the detailed crystallization process of
389 anhydrous trehalose, the formation and melting of the individual forms of crystals will
390 need to be examined.

391

392 **Acknowledgement**

393

394 This work was supported by a Grant-in-Aid for Science Research (B) (No.
395 19H02499) and challenging Exploratory Research (No. 15K14206) from the Ministry
396 of Education, Science, Sport and Culture of Japan, and the Toyo Institute of Food
397 Technology.

398

399 **References**

400

401 Abdul-Fattah, A. M., Truong-Le, V., Yee, L., Nguyen, L., Kalonia, D. S., Cicerone, M.
402 T., Pikal, M. J., 2007. Drying-induced variations in physico-chemical properties of

403 amorphous pharmaceuticals and their impact on stability (I): Stability of a monoclonal
404 antibody. *J. Pharm. Sci.*, 96 (8), 1983-2008.

405 Avrami, M., 1939. Kinetics of phase change. I General theory. *J. Chem. Phys.*, 7 (12),
406 1103-1112.

407 Avrami, M., 1940. Kinetics of phase change. II Transformation- time relations for
408 random distribution of nuclei. *J. Chem. Phys.*, 8 (2), 212-224.

409 Avrami, M., 1941. Granulation, phase change, and microstructure Kinetics of phase
410 change. III. *J. Chem. Phys.*, 9 (2), 177-184.

411 Boyer, R. F., Spencer, R. S., 1944. Thermal expansion and second- order transition
412 effects in high polymers: Part I. Experimental results. *J. Appl. Phys.*, 15, 398-405.

413 Cai, X., Seidl, I., Mu, W., Zhang, T., Stressler, T., Fischer, L., Jiang, B., 2018.
414 Biotechnical production of trehalose through the trehalose synthase pathway: current
415 status and future prospects. *Appl. Microbiol. Biotechnol.*, 102 (7), 2965–2976.

416 Crowe, J. H., 2007. Trehalose as a “chemical chaperone”: Fact and fantasy. *Adv. Exp.*
417 *Med. Biol.*, 594, 143-158.

418 Elbein, A. D., Pan, Y. T., Pastuszak, I., Carroll, D., 2003. New insights on trehalose: a
419 multifunctional molecule. *Glycobiol.*, 13 (4), 17R–27R.

420 Erofeev, B. V., 1946. Generalized equation of chemical kinetics and its application in
421 reactions involving solids. *Compt. Rend. Acad. Sci. USSR*, 52 (6), 511-514.

422 Frenkel, J. “*Kinetic Theory of Liquids*,” 1955. Oxford Univ. Press, London.

423 Hidaka, F., Sato, T., Fujioka, A., Takeda, K., Imanaka, H., Ishida, N., Imamura, K., 2019.
424 Controlling the drying process in vacuum foam drying under low vacuum conditions by
425 inducing foaming by needle stimulation of the solution. *Dry. Technol.*, 37 (12),
426 1520–1527.

427 Hurta, M., Pitkanen, I., Knuutinen, J., 2004. Melting behaviour of D-sucrose,
428 D-glucose and D-fructose. *Carbohydr. Res.*, 339 (13), 2267-2273.

429 Imamura, K., Sakaura, K., Ohyama, K., Fukushima, A., Imanaka, H., Sakiyama, T.,
430 Nakanishi, K., 2006. Temperature scanning FTIR analysis of hydrogen bonding states
431 of various saccharides in amorphous matrixes below and above their glass transition
432 temperatures. *J. Phys. Chem. B*, 110 (31), 15094-15099.

433 Imamura, K., Maruyama, Y., Tanaka, K., Yokoyama, T., Imanaka, H., Nakanishi, K.,
434 2008a. True density analysis of a freeze-dried amorphous sugar matrix. *J. Pharm. Sci.*,
435 97 (7), 2789–2797.

436 Imamura, K., Asano, Y., Maruyama, Y., Yokoyama, T., Nomura, M., Ogawa, S.,
437 Nakanishi, K., 2008b. Characteristics of hydrogen bond formation between sugar and
438 polymer in freeze-dried mixtures under different rehumidification conditions and its

439 impact on the glass transition temperature. *J. Pharm. Sci.*, 97 (3), 1301-1312.

440 Imamura, K., Ohyama, K., Yokoyama, T., Maruyama, Y., Imanaka, H., Nakanishi, K.,
441 2008c. Temperature scanning FTIR analysis of interactions between sugar and polymer
442 additive in amorphous sugar-polymer mixtures. *J. Pharm. Sci.*, 97 (1), 519-28.

443 Imamura, K., Nomura, M., Tanaka, K., Kataoka, N., Oshidani, J., Imanaka, H.,
444 Nakanishi, K., 2010. Impacts of compression on crystallization behavior of freeze-dried
445 amorphous sucrose. *J. Pharm. Sci.*, 99 (7), 1452-1463.

446 Imamura, K., Kagotani, R., Nomura, M., Kinugawa, K., Nakanishi, K., 2012.
447 Heterogeneity of the state and functionality of water molecules sorbed in an amorphous
448 sugar matrix. *Carbohydr. Res.*, 351 (1), 108-113.

449 Imamura, K., Kinugawa, K., Kagotani, R., Nomura, M., Nakanishi, K., 2012. Impacts
450 of compression, physical aging, and freezing rate on the crystallization characteristics of
451 an amorphous sugar matrix. *J. Food Eng.*, 112 (4), 313-318.

452 Jain, N. K., Roy, I., 2009. Effect of trehalose on protein structure. *Protein Sci.*, 18(1),
453 24-36.

454 Kagotani, R., Kinugawa, K., Nomura, M., Imanaka, H., Naoyuki, I., Imamura, K., 2013.
455 Improving the physical stability of freeze-dried amorphous sugar matrices by
456 compression at several hundreds MPa. *J. Pharm. Sci.*, 102 (7), 2187-2197.

457 Kedward, C. J., MacNaughtan, W., Blandshard, J. M. V., Mitchell, J. R., 2008.
458 Crystallization kinetics of lactose and sucrose based on isothermal differential scanning
459 calorimetry. *J. Food Sci.*, 63 (2), 192-197.

460 Kedward, C. J., MacNaughtan, W., Mitchell, J. R., 2000. Isothermal and non-isothermal
461 crystallization in amorphous sucrose and lactose at low moisture contents. *Carbohydr.*
462 *Res.*, 329 (2), 423-430.

463 Kinugawa, K., Kinuhata, M., Kagotani, R., Imanaka, H., Ishida, N., Kitamatsu, M.,
464 Nakanishi, K., Imamura, K., 2015. Inhibitory effects of additives and heat treatment on
465 the crystallization of freeze-dried sugar. *J. Food Eng.*, 155, 37-44.

466 Kopjar, M., Hribar, J., Simcic, M., Zlatić, E., Pozrl, T., Pilizota, V., 2013) Effect of
467 trehalose addition on volatiles responsible for strawberry aroma. *Nat. Prod. Commun.*,
468 8(12), 1767-1770.

469 Kubota, M., Sawatani, I., Oku, K., Takeuchi, K., Murai, S., 2004. The development of
470 α,α -trehalose production and its application (in Japanese. *J. Appl. Glycosci.*, 51, 63-70.
471 [The Merck index, 10th ed. Rahway, NJ, Merck & Co., Inc., p. 34, and p. 865.](#)

472 Miller, D. P., de Pablo, J. J., 2000. Calorimetric solution properties of simple
473 saccharides and their significance for the stabilization of biological structure and
474 function. *J. Phys. Chem. B*, 104 (37), 8876-8883.

475 Nagase, H., Endo, T., Ueda, H., Nagasaki, M., 2002. An anhydrous polymorphic form
476 of trehalose. *Carbohydr. Res.*, 337 (2), 167-173.

477 Nagase, H., Ogawa, N., Endo, T., Shiro, M., Ueda, H., Sakurai, M., 2008. Crystal
478 structure of an anhydrous form of trehalose: structure of water channels of trehalose
479 polymorphism. *J. Phys. Chem. B*, 112 (30), 9105-9111.

480 Neri, L., Hernando, I., Pérez-Munuera, I., Sacchetti, G., Mastrocola, D., Pittia, P., 2014.
481 Mechanical properties and microstructure of frozen carrots during storage as affected by
482 blanching in water and sugar solutions. *Food Chem.*, 144, 65–73.

483 Ohashi, T., Yoshii, H., Furuta, T., 2007a. Effect of drying methods on crystal
484 transformation of trehalose. *Dry. Technol.*, 25 (7-8), 1305-1311.

485 Ohashi, T., Yoshii, H., Furuta, T., 2007b. Innovative crystal transformation of dihydrate
486 trehalose to anhydrous trehalose using ethanol. *Carbohydr. Res.*, 342(6), 819-25.

487 Ohtake, S., Wang, Y. J., 2011. Trehalose: Current use and future applications. *J. Pharm.*
488 *Sci.*, 100 (6), 2020-2053.

489 Pyszczynski, S. J., Munson, E. J., 2013. Generation and characterization of a new solid
490 form of trehalose. *Mol. Pharm.*, 10 (9), 3323-3332.

491 Takeda, K., Sekitoh, T., Fujioka, A., Yamamoto, K., Okamoto, T., Matsuura, T., Imanaka,
492 H., Ishida, N., Imamura, K., 2019. Physical stability of an amorphous sugar matrix dried
493 from methanol as an amorphous solid dispersion carrier and the influence of heat
494 treatment. *J. Pharm. Sci.*, 108 (6), 2056-2062.

495 Umene, S., Hayashi, M., Kato, K., Masunaga, H., 2015. Physical properties of root
496 crops treated with novel softening technology capable of retaining the shape, color, and
497 nutritional value of foods. *Dysphagia*, 30(2), 105–113.

498 Verhoeven, N., Neoh, T. L., Furuta, T., Yamamoto, C., Ohashi, T., Yoshii, H., 2012.
499 Characteristics of dehydration kinetics of dihydrate trehalose to its anhydrous form in
500 ethanol by DSC. *Food Chem.*, 132 (4), 1638-1643.

501 Walayat, N., Xiong, H. G., Xiong, Z. Y., Moreno, H. M., Nawaz, A., Niaz, N.,
502 Randhawa, M. A., 2020. Role of cryoprotectants in surimi and factors affecting surimi
503 gel properties: A review. *Food Rev. Int.*, *in press*

504 Wang, Y., Truong, T., Glass transition and crystallization in foods. in “Non-equilibrium
505 states and glass transitions in foods: Processing effects and product-specific
506 implications,” pp. 153-172, edited by B. Bhandari and Y. H. Roos, Woodhead
507 Publishing, Cambridge, MA, 2017.

508 Wolkers, W. F., van Kilsdonk, M. G., Hoekstra, F. A., 1998. Dehydration-induced
509 conformational changes of poly-L-lysine as influenced by drying rate and carbohydrates.
510 *Biochim. Biophys. Acta*, 1425 (1), 127-136.

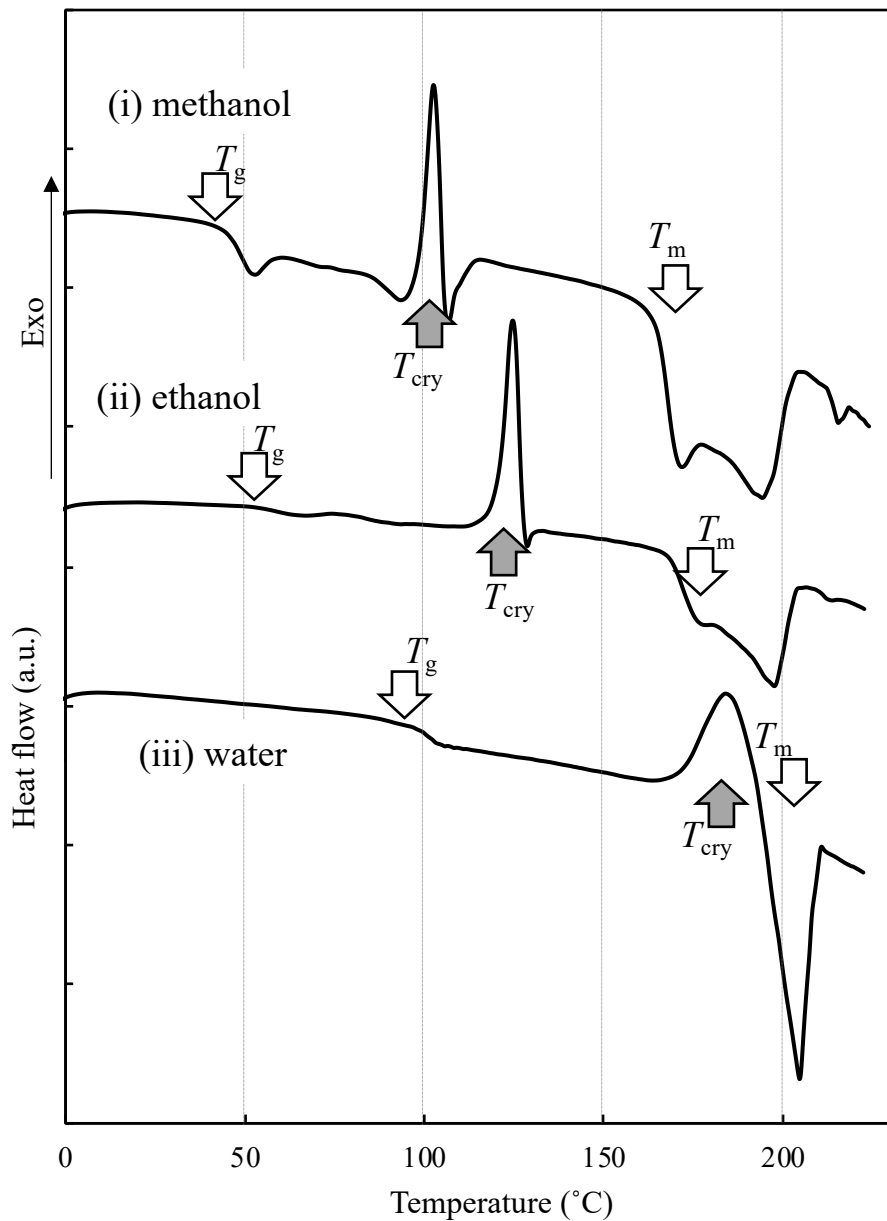


Fig. 1. DSC thermograms for amorphous trehalose matrices, vacuum-foam dried from (i) methanol and (ii) ethanol and (iii) for freeze-dried aqueous trehalose solutions. Arrows in the graph denote T_g , T_{cry} , and T_m .

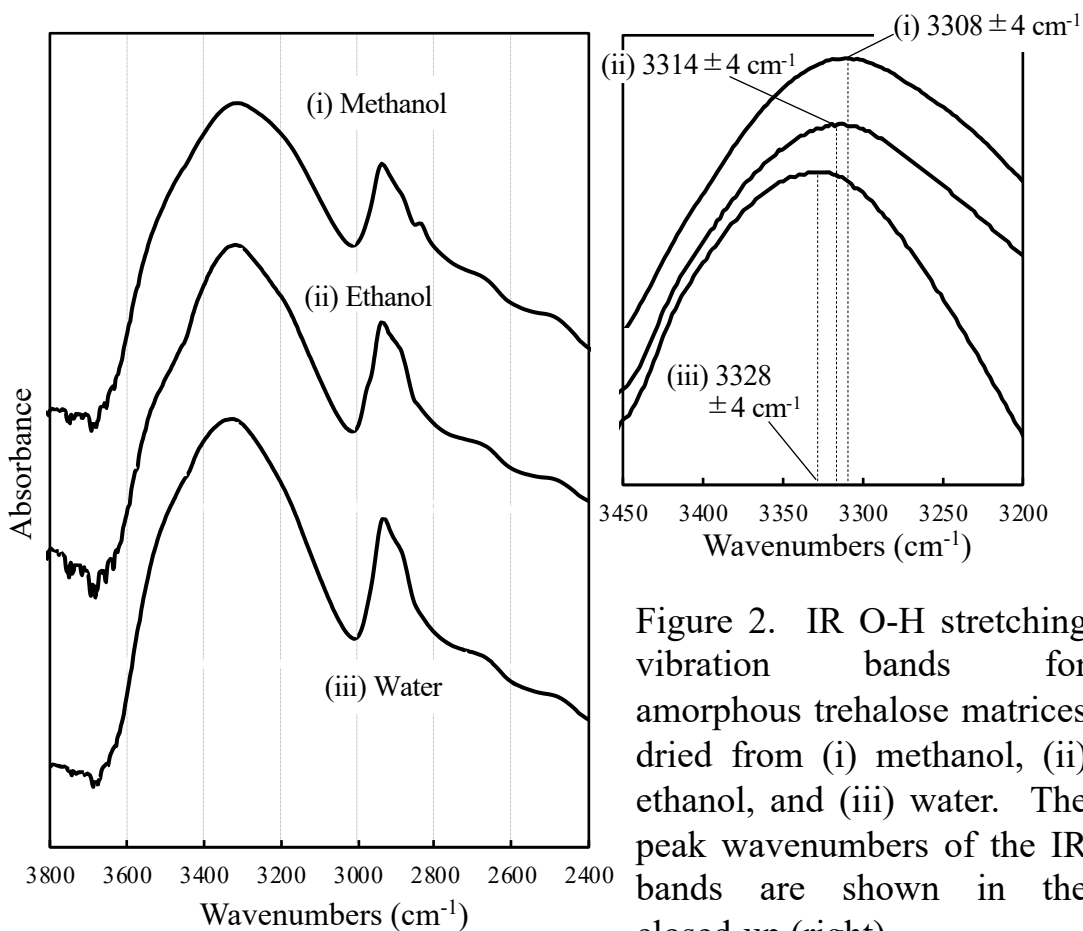


Figure 2. IR O-H stretching vibration bands for amorphous trehalose matrices, dried from (i) methanol, (ii) ethanol, and (iii) water. The peak wavenumbers of the IR bands are shown in the closed-up (right).

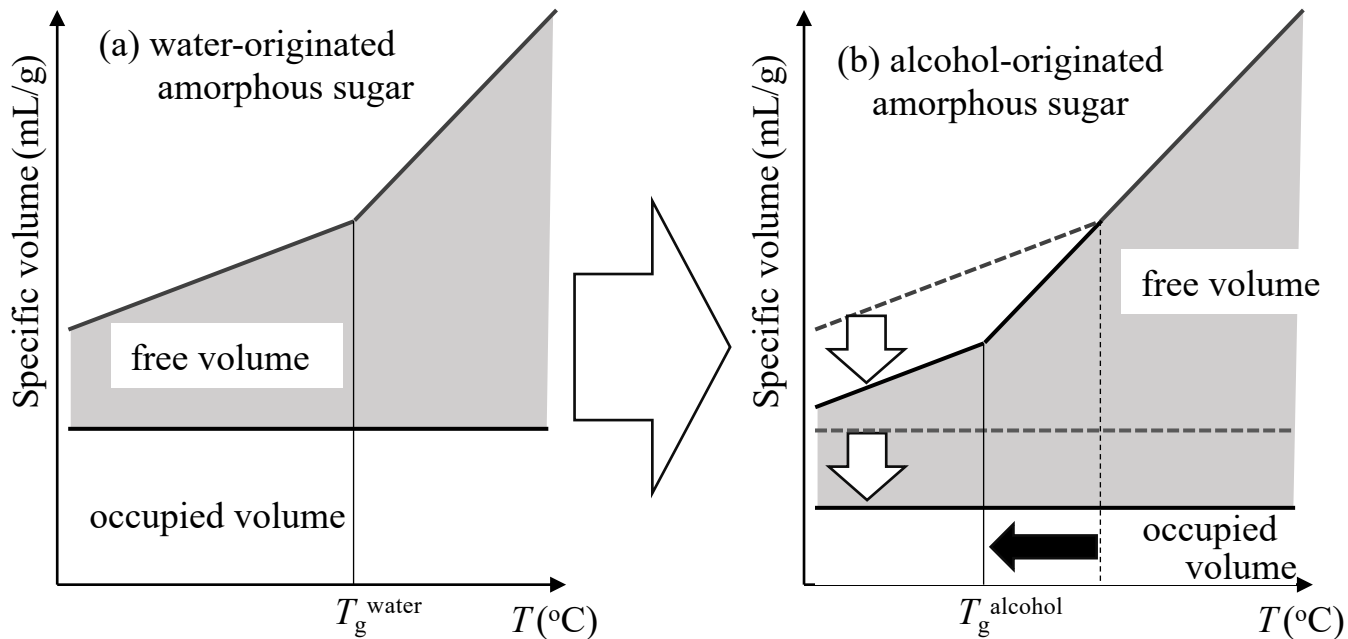


Fig. 3. Schematic relationship between temperature and the specific volume of an amorphous sugar matrix, dried from (a) water or (b) alcohol. According to free volume theory (Boyer & Spencer, 1944; Frenkel, 1955), the sugar specific volume is comprised of an occupied volume and a free volume. The free volume increases with increasing temperature, and the occupied volume for the alcohol-originated amorphous sugar appears to be markedly smaller than that for the water-originated one.

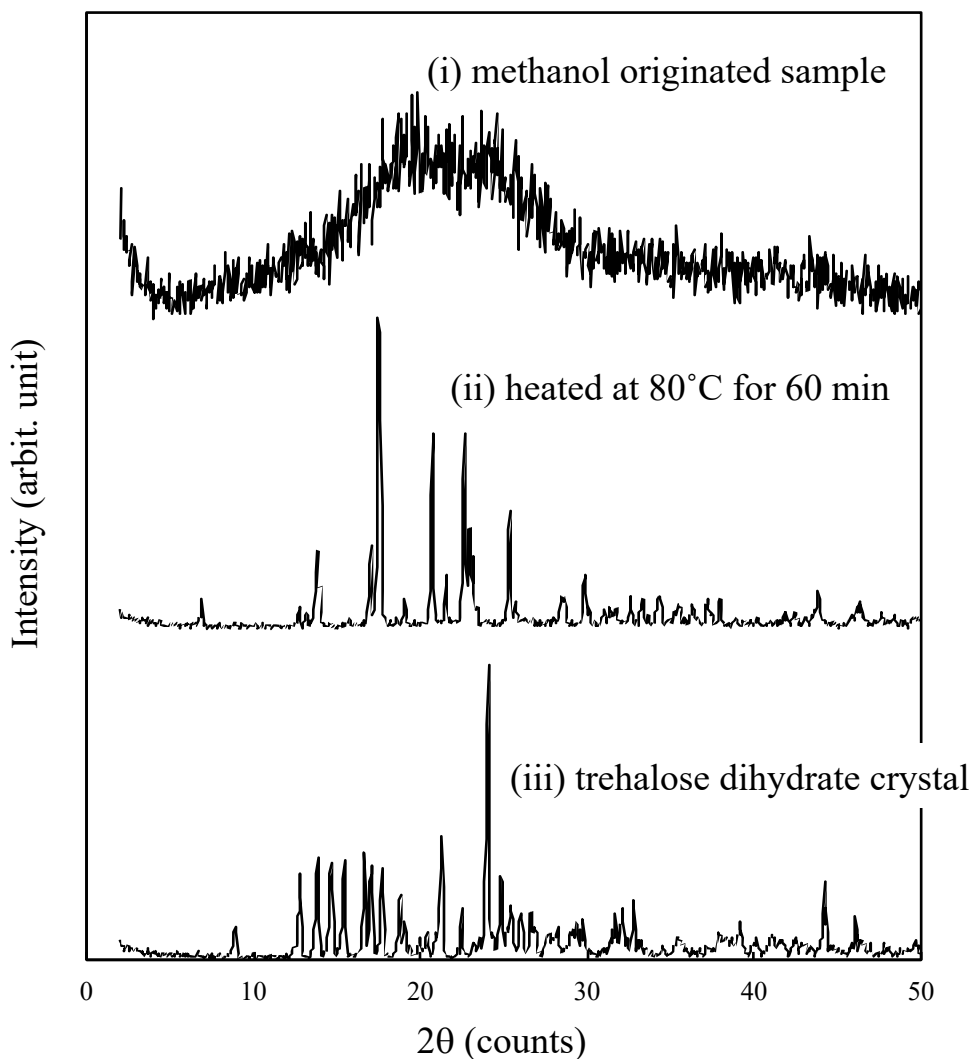


Fig. 4. X-ray diffraction patterns of trehalose samples that had been vacuum foam dried from methanol (i) and then heated at 80°C for 60 min (ii) as well as trehalose dihydrate crystal (iii).

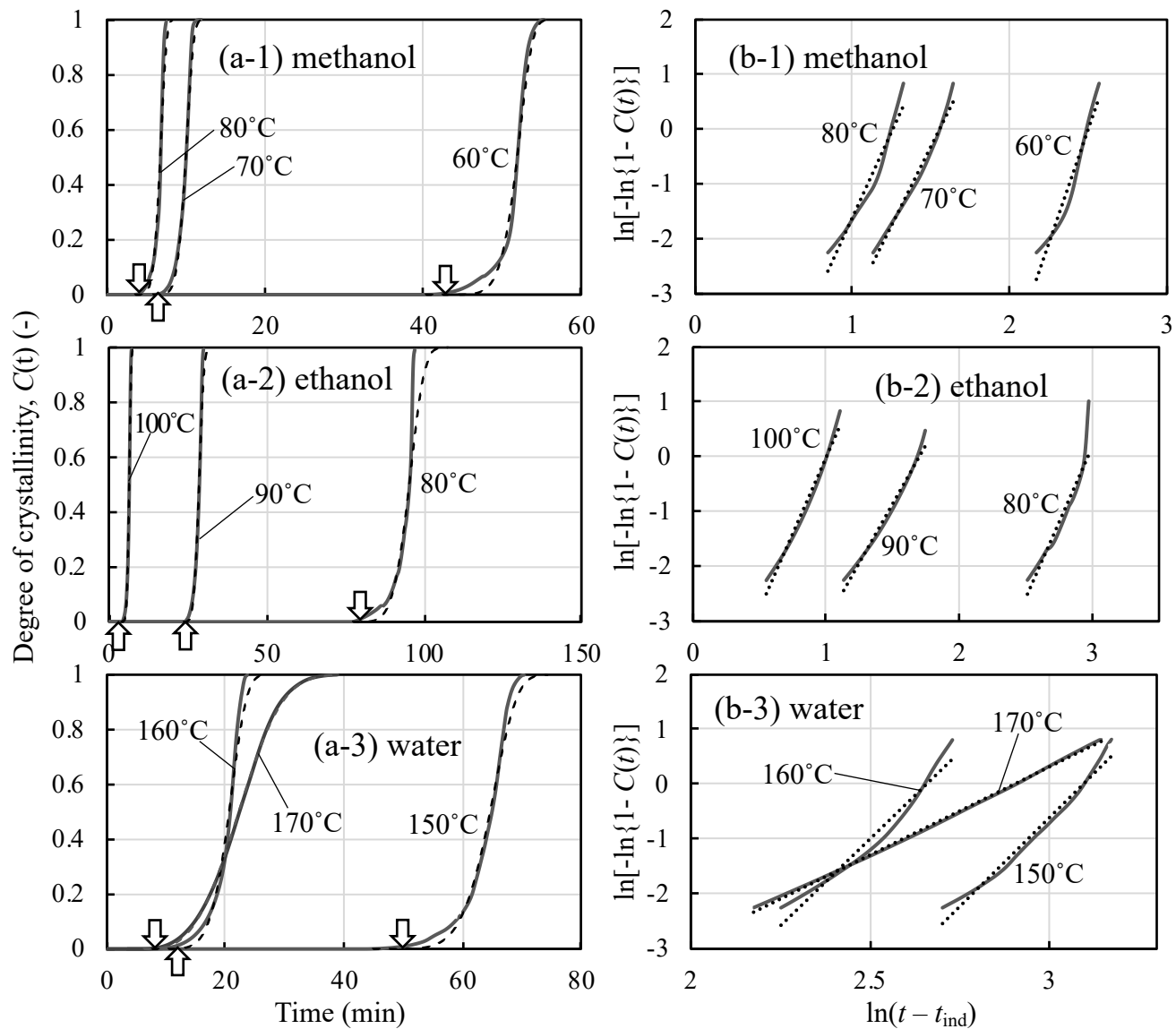


Fig. 5. Isothermal crystallization of amorphous trehalose, vacuum foam dried from (a-1) methanol and (b-1) ethanol, at different temperatures and their Avrami plots (b-1, 2). Results for the trehalose sample obtained by freeze-drying from water were also shown (a-3, b-3). Arrows in graphs (a-1~3) indicate the induction times, t_{ind} , and dotted lines in graphs (a-1~3) and (b-1~3) are the approximated ones.

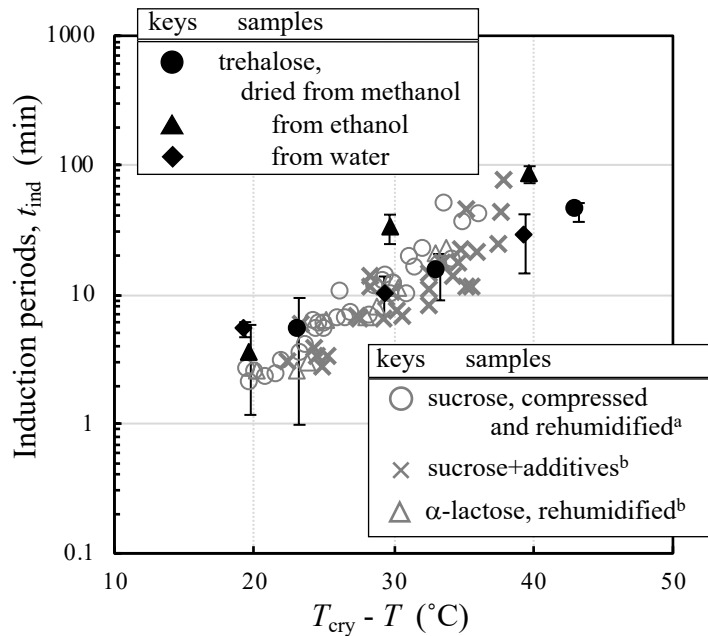


Fig. 6. Relationship between induction periods, t_{ind} , and crystallization temperature, T_{cry} . T refers to the temperature in the isothermal crystallization test. The values for the sucrose and α -lactose samples (gray keys) are cited from our previous reports (^a Imamura, Kinugawa, Kagotani, Nomura, & Nakanishi, 2012; ^b Kinugawa et al., 2015).

1 **Table 1**
 2 **Temperatures and enthalpies for crystallization (T_{cry} , ΔH_{cry}) of amorphous**
 3 **trehalose and melting (T_{m} , ΔH_{m}) as well as the T_{g} values. The amorphous**
 4 **trehalose samples were prepared by being dried from different solvents (methanol,**
 5 **ethanol, and water).**

Solvent	T_{g} ($^{\circ}\text{C}$)	T_{cry} ($^{\circ}\text{C}$)	ΔH_{cry} (J/g)	T_{m} ($^{\circ}\text{C}$)	ΔH_{m} (J/g)
Methanol	44 ± 2	103 ± 5	47 ± 8	177 ± 7	156 ± 10
Ethanol	56 ± 3	120 ± 8	52 ± 8	178 ± 10	141 ± 14
Water	107 ± 6 105^{a} , $115^{\text{b,d}}$ 100^{c} , 117^{e}	184 ± 6 189^{c} , 185^{f} 180^{g}	24 ± 9 140^{e}	208 ± 2 $215^{\text{e,g}}$ 213^{f}	24 ± 10 $156^{\text{h,i}}$

6 ^a Imamura et al., 2008c; ^b Miller & de Pablo, 2000; ^c Roos, 1993;

7 ^d Saleki-Gerhardt & Zograf, 1994; ^e Surana, Pyne, & Suryanarayanan, 2004;

8 ^f Pyszczyński & Munson, 2013; ^g Sussich, Urbani, Princivalle, & Cesàro, 1998;

9 ^h Cai et al., 2018; ⁱ Jain & Roy, 2009

10

1 **Table 2**
 2 **Induction time (t_{ind}), apparent crystallization rate constants (k_{cry}), and Avrami**
 3 **constants (n), determined from isothermal crystallization processes of amorphous**
 4 **trehalose, dried from different solvents (methanol, ethanol, and water), at different**
 5 **temperatures**

Solvent	Temp. (°C)	t_{ind} (min)	k_{cry} (min ⁻¹)	n (-)
Methanol	60	44 ± 7	0.104 ± 0.070	5.9 ± 2.3
	70	15 ± 6	0.188 ± 0.034	5.5 ± 0.6
	80	5.2 ± 4.2	0.395 ± 0.297	5.8 ± 0.4
Ethanol	80	85 ± 13	0.064 ± 0.018	4.3 ± 1.4
	90	33 ± 8	0.181 ± 80.007	5.2 ± 1.4
	100	3.5 ± 2.3	0.436 ± 0.097	4.8 ± 1.1
Water	150	28 ± 14	0.040 ± 0.007	5.2 ± 1.2
	160	10 ± 3	0.055 ± 0.018	5.2 ± 1.1
	170	5.4 ± 0.7	0.045 ± 0.016	3.2 ± 0.4

Conflict of interest: No conflicting relationship exists for any author.

Author Name: Takanari Sekitoh, Takashi Okamoto, Akiho Fujioka, Tomohiko Yoshioka, Shinji Terui, Hiroyuki Imanaka, Naoyuki Ishida, and Koreyoshi Imamura

Title of Article: Crystallization Characteristics of Amorphous Trehalose Dried from Alcohol

Manuscript Number:

Date:

July 11th, 2020.

1 **Figure legends**

2

3 Fig. 1. DSC thermograms for amorphous trehalose matrices, vacuum-foam dried from
4 (i) methanol and (ii) ethanol and (iii) for freeze-dried aqueous trehalose solutions.
5 Arrows in the graph denote T_g , T_{cry} , and T_m .

6

7 Figure 2. IR O-H stretching vibration bands for amorphous trehalose matrices, dried
8 from (i) methanol, (ii) ethanol, and (iii) water. The peak wavenumbers of the IR bands
9 are shown in the closed-up (right).

10

11 Fig. 3. Schematic relationship between temperature and the specific volume of an
12 amorphous sugar matrix, dried from (a) water or (b) alcohol. According to free
13 volume theory (Boyer & Spencer, 1944; Frenkel, 1955), the sugar specific volume is
14 comprised of an occupied volume and a free volume. The free volume increases with
15 increasing temperature, and the occupied volume for the alcohol-originated amorphous
16 sugar appears to be markedly smaller than that for the water-originated one.

17

18 Fig. 4. X-ray diffraction patterns of trehalose samples that had been vacuum foam dried
19 from methanol (i) and then heated at 80°C for 60 min (ii) as well as trehalose dihydrate
20 crystal (iii).

21

22 Fig. 5. Isothermal crystallization of amorphous trehalose, vacuum foam dried from
23 (a-1) methanol and (b-1) ethanol, at different temperatures and their Avrami plots (b-1,
24 2). Results for the trehalose sample obtained by freeze-drying from water were also
25 shown (a-3, b-3). Arrows in graphs (a-1~3) indicate the induction times, t_{ind} , and
26 dotted lines in graphs (a-1~3) and (b-1~3) are the approximated ones.

27

28 Fig. 6. Relationship between induction periods, t_{ind} , and crystallization temperature, T_{cry} .
29 T refers to the temperature in the isothermal crystallization test. The values for the
30 sucrose and α -lactose samples (gray keys) are cited from our previous reports (Imamura,
31 Kinugawa, Kagotani, Nomura, & Nakanishi, 2012; Kinugawa et al., 2015).

32

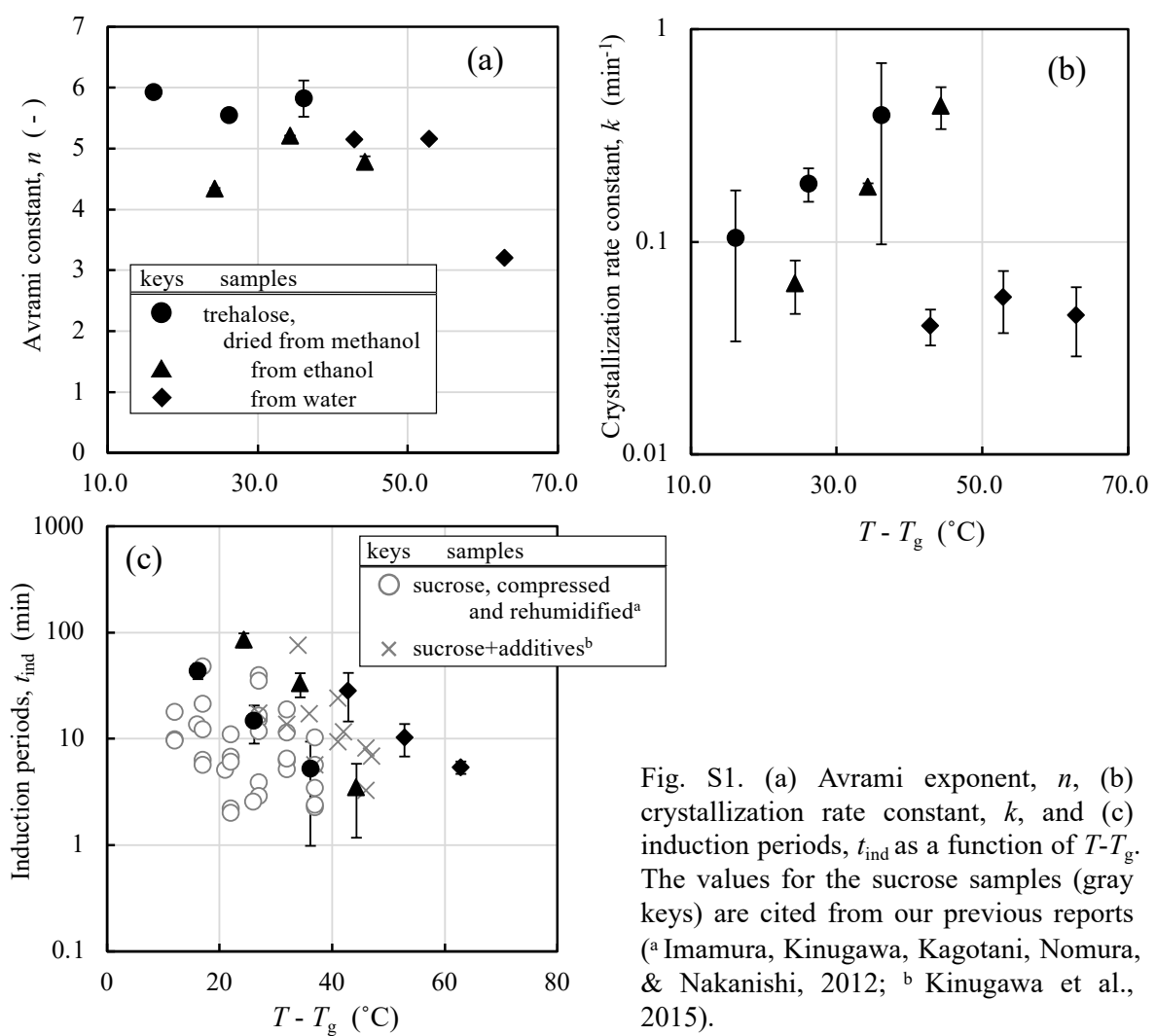


Fig. S1. (a) Avrami exponent, n , (b) crystallization rate constant, k , and (c) induction periods, t_{ind} as a function of $T - T_g$. The values for the sucrose samples (gray keys) are cited from our previous reports (^aImamura, Kinugawa, Kagotani, Nomura, & Nakanishi, 2012; ^bKinugawa et al., 2015).

Takanari Sekitoh: Methodology, Validation, Investigation, Writing-Original Draft

Takashi Okamoto: Validation, Investigation, Visualization

Akiho Fujioka: Methodology, Visualization

Tomohiko Yoshioka: Methodology, Investigation, Visualization

Shinji Terui: Validation, Investigation

Hiroyuki Imanaka: Resources, Validation

Naoyuki Ishida: Conceptualization, Methodology, Validation, Investigation

Koreyoshi Imamura: Conceptualization, Supervision, Writing-Review & Editing